Scientific Bulletin of the
Politehnica University of Timisoara
Transactions on Mechanics
Special issue

2nd Workshop on
Vortex Dominated Flows
Bucharest, Romania
June 30 – July 1, 2006

AUTOMATED PROCEDURE FOR DESIGN AND 3D NUMERICAL ANALYSIS OF THE FLOW THROUGH IMPELLERS

Teodor MILOŞ, Assoc. Prof. *
Department of Hydraulic Machinery
"Politehnica" University of Timisoara

Sebastian MUNTEAN, Senior Researcher*
Center of Advanced Research in Engineering Sciences
Romanian Academy - Timisoara Branch

Adrian STUPARU, Assist. Prof.
Department of Hydraulic Machinery
"Politehnica" University of Timisoara

Alexandru BAYA, Assoc. Prof.
Department of Hydraulic Machinery
"Politehnica" University of Timisoara

Romeo SUSAN-RESIGA, Prof.
Department of Hydraulic Machinery
"Politehnica" University of Timisoara

**Corresponding author*: Bv Mihai Viteazu 24, 300223, Timisoara, Romania
Tel.: (+40) 256 403681, Fax: (+40) 256 403682, Email: tmilos@mh.mec.upt.ro

ABSTRACT

The present paper presents a fully automated procedure for generating the inter-blade channel 3D geometry for impeller, starting with the geometrical data provided by the quasi- 3D code. The 3D domain is generated in GAMBIT with a specialized script, and then it is automatically discretized. All inlet/outlet, solid and periodic boundaries are specified for a standard topology of the inter-blade channel. Although GAMBIT has a module, called G-TURBO, specialized in turbomachinery analysis, it has been found that for highly distorted geometries specific to axial-radial machines the results are not satisfactory. This is why we developed an original procedure that successfully addresses all geometrical particularities of centrifugal pumps, Francis turbines, and pump-turbines. The paper describes the implementation of our procedure, and a few examples of 3D flow analysis in impellers.

KEYWORDS

automated procedure for design, impellers, 3D numerical analysis

NOMENCLATURE

Q	[m^3/s]	discharge
H	[m]	head
M	[Nm]	torque
z	[-]	number of blades
n	[rpm]	speed
n_q	[]	characteristic speed
g	[m/s^2]	gravity
rv_u	[m^2/s^2]	hydraulic momentum
β	[°]	relative flow angle
φ	[°]	wrapping blade angle
v, V	[m/s]	absolute velocity
W	[m/s]	relative velocity
D	[m]	diameter
r, R	[m]	radius

Subscripts and Superscripts

r	radial direction
θ	circumferential direction
z	axial direction
in	interior
ex	exterior
ps	pressure side
ss	suction side
m	meridian
x	curvilinear coordinate

1. INTRODUCTION

The intermediary way between inlet and outlet results by interpolation one of the significant kinematics function for distribution of the blade loading over the impeller channels. The interpolation is made along the streamlines controlled through the curvilinear coordinate "x" and not by the current radius "r" because loading is better quantified in the mixed zone. The hydraulic momentum is the function, which reflects blade loading between inlet and outlet. For a current point heaving the curvilinear coordinate "x" it is like [1]:

$$M_{hx} = \rho Q_t \left(r_x v_{ux} - r_1 v_{u1} \right) \tag{1}$$

From (1) developing $(rv_u)_x$ results:

$$\left(rv_u \right)_x = r_1 v_{u1} + \frac{M_{hx}}{\rho Q_t} = f(x) \tag{2}$$

The function directly linked to the hydraulic momentum is $\Delta(rv_u)$, therefore by controlling the variation along the impeller channel of the product rv_u, results the variation of the hydraulic momentum with the radius, repartition of partial head, and distribution of the pressure differences on the blade sides. The variation of the rv_u product implies the variation of the relative flow angle β required by the blade construction in the hypothesis that the relative speed is tangent at the surface of the blade. The height of the velocity triangles is given by the meridian velocity v_m, corrected with the obstruction factor given by the thickness of the blades. If we consider a current point on the stream line marked with "i", then the current angle β_i results from equation:

$$\beta_i = arctg\left(\frac{v_{mi}}{\rho_i} \frac{1}{u_i - v_{ui}} \right) \tag{3}$$

We observe that in (3) appear the factors r_i ($u_i = r_i \omega$) and v_{ui}, therefore indifferent of the two variants interpolate we obtain the same type of information. The best choice is that β angle to be directly linked of the blade orientation in the rotor channel. The variation of the β angle between inlet and outlet must be chosen in such a way that blade loading is relatively uniform and the variation is rising strictly on the entire domain. For a better engagement of the stream at inlet and outlet it is recommended that in the vicinity of the limit points the blade to be made as an inactive blade. By analyzing many rotors there are established that this condition is realized if the variation curves of β has a zero derivate at inlet and outlet.

In this case, two possible solutions have been chosen:

a) Interpolation with two connected parabola arcs,
b) Interpolation with two parabola arcs connected by a straight segment line.

2. INTERPOLATION WITH TWO CONNECTED PARABOLA ARCS

In the first case, the connection of two parabola arcs is made after common tangent at the point x_3. The function which defines the two parabola arcs with vertically focus axes is noted with f_1 and f_2 and is expressed by the general equations:

$$\begin{cases} f_1(x) = a_1 x^2 + b_1 x + c_1 \\ f_2(x) = a_2 x^2 + b_2 x + c_2 \end{cases} \tag{4}$$

We observe that for a correct definition it is necessary to know the coefficients a_1, b_1, c_1, a_2, b_2, c_2. Therefore, we need six equations with six variables resulting from the equations (4). Putting analytical conditions of position and connection we will have in accordance with Fig. 1. analytical translating the six conditions will result a six equations system with six variables (5), which is exactly solved by Gauss eliminating algorithm.

$$\begin{cases} f_1'(x_3) = f_2'(x_3) & \text{(I)} \\ f_1'(x_1) = 0 & \text{(II)} \\ f_2'(x_2) = 0 & \text{(III)} \\ f_1(x_3) = f_2(x_3) & \text{(IV)} \\ f_1(x_1) = \beta_1 & \text{(V)} \\ f_2(x_2) = \beta_2 & \text{(VI)} \end{cases} \tag{5}$$

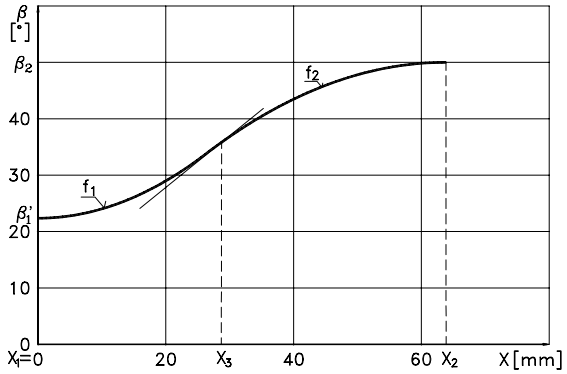

Fig.1 β interpolation with two parabola arcs direct connected

3. INTERPOLATION WITH TWO PARABOLAS ARCS CONNECTED BY A STRAIGHT SEGMENT LINE

In the second case, the connection of two parabola arcs is made by a straight segment line, at the points x_3, respectively x_4. The function which defines the two parabola arcs with vertically focus axes is noted with f_1, f_2 and the straight segment line f_3, heaving general equations:

$$\begin{cases} f_1(x) = a_1 x^2 + b_1 x + c_1 \\ f_2(x) = a_2 x^2 + b_2 x + c_2 \\ f_3(x) = mx + n \end{cases} \tag{6}$$

It can be observed, that for a correct definition is necessary to know the coefficients a_1, b_1, c_1, a_2, b_2, c_2, m, n. Therefore, we need eight equations with eight variables resulting from the equations (6). Analytical translating the eight conditions will result an eight equations system with eight variables (7) that is exactly solved by Gauss eliminating algorithm.

$$\begin{cases} f_1(x_1) = \beta_1' & \text{(I)} \\ f_2(x_2) = \beta_2 & \text{(II)} \\ f_1(x_3) = f_3(x_3) & \text{(III)} \\ f_2(x_4) = f_3(x_4) & \text{(IV)} \\ f_1'(x_1) = 0 & \text{(V)} \\ f_2'(x_2) = 0 & \text{(VI)} \\ f_1'(x_3) = m & \text{(VII)} \\ f_2'(x_4) = m & \text{(VIII)} \end{cases} \tag{7}$$

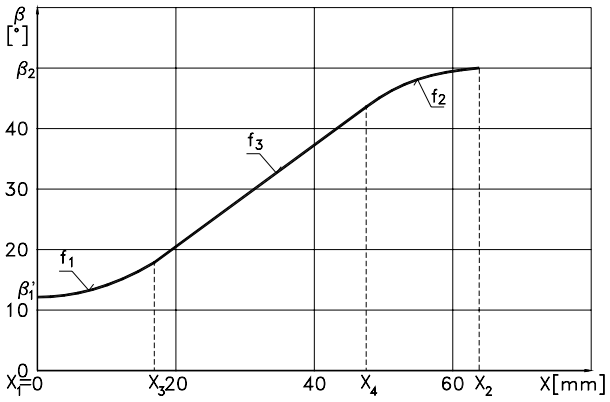

Fig. 2. Relative flow angle β interpolation with two parabola arcs connected by a straight segment line

4. BLADE CALCULUS IN PROJECTION ON A PLANE PERPENDICULAR ON THE ROTATION AXIS

In booth cases, it is possible to modify the points position x_3 or x_4 on the interval (x_1,x_2) until is found an optimum variation for the blade shape. The projection image on a perpendicular plane on the rotation axes is calculated and represented in polar coordinates system (r,φ), where r is the radius point from the streamline and φ is the wrapping angle of the blade, measured between entry and exit. The φ angle is evaluated with the equation:

$$\varphi = \int_{x\_in}^{x\_ex} \frac{dx}{r \cdot tg\,\beta} \tag{8}$$

The integration is done numerically by summing the partial surfaces using the trapeze method. From hydrodynamic field calculation can result 3 to11 or more streamlines. Applying formula (8) for each streamline it will result a φ_{max} angle. Using relation (8) for the wrapping angle of the blade calculus, φ_{ij} (in 3D is identified with θ variable of cylindrical reference coordinate system (r, θ, z)) where i – controls current point along a streamline, j – controls the number of streamlines, leads to some independent results, so that at the end when they are assembled in a blade frame surface, it can result with swirls on width, which from a hydraulic point of view is unacceptable. From that is necessary a strategy in order to solve the problem, which consist of imposing some supplementary conditions. These conditions are a function of impeller type characterized by n_q. For radial impeller with $n_q < 40$ (I) the solution is possible by a specific modality, and for $n_q > 40$ (II) the solution is completed by supplementary aspects.

If the radial extension of the impellers is reduced $D_2/D_0 < 2$ the blades will occupy a great part of the passing zone of axial flow to radial flow (the curvature zone of the hydrodynamic field domain).

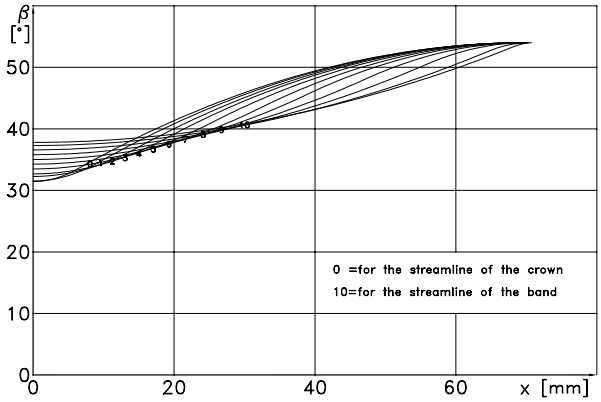

Fig. 3. Distribution of relative flow angle β on streamlines for the impeller with n_q=18.18

The construction angles of the blades at inlet are frequently over 20°, but at outlet are necessary angles of about 40°. Therefore the angular interval from inlet to outlet is about 20°, case (II), different from case (I) when this interval is about 40°…50°. The manipulating interval for angle β is thus greatly reduced. The optimum positioning of leading edge in the purpose to relatively equalize the length of the streamlines in the blade area does not offer sensible changes of the maximum wrapping angle of the blade. This it also observed from the structure of calculus relation (8) where the variable r, the current radius on the streamline, has

a much reduced variation domain. So, we are in the situation that the optimization for the equalization of wrapping angle φ_{max} at crown is with 20°…30° grater than φ_{max} from band. In this way, after optimization of positioning of leading edge and trailing edge, remains to find an optimum of β angle variation for all streamlines in a sense that the percentage position of points x_3 respectively x_3 and x_4 is the same for all streamlines. We will thus have a relationship between them which has a result in a smooth shape of blade camber surface. The second target of optimization is to reduce the blade torsion between inlet and outlet. It can be observed that at inlet the blade is inclined in the rotor channel.

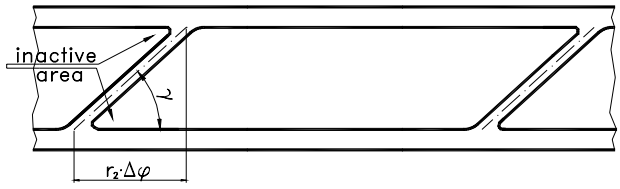

Fig. 4. Lean angle of the blade impeller at the outlet.

If we impose the condition that the trailing edge to be parallel with the rotation axis will result torsion of the blade in the interblade channel of impeller.

In order to attenuate the torsion we will impose at the outlet a lean angle of the blade, but no less then 45° ($\gamma > 45°$, Fig. 4) because otherwise will appear inactive areas at the connection of the blade surface with the band and crown surface. In projection, the blade inclination will appear as an angular difference $\Delta\varphi$ proportional for each streamline, so that the leading edge too will be proportionally rotated with this angular difference $\Delta\varphi$, which as an effect will reduce the leading edge inclination in the rotor channel and implicitly will reduce the blade torsion between entrance and exit.

5. TRANSPOSITION OF THE GEOMETRIC DATA OF THE PUMP BLADE IN THE CONFORMAL MAPPING PLAN

After the computer aided design of the impeller blade using the method presented above, the 3D camber surface of the blade and the band and crown surfaces for the leading of the fluid to the blade zone, the blade zone and after the blade zone is obtained. For the numerical computation using FLUENT it is needed that the frame surface of the blade to be completed with a thickness function which will generate the suction side and pressure side afterwards. For this operation the most efficient and precise method is the conformal transformation mapping method. First the camber line of the blade is transpose to the conformal mapping plan. If x is the curvilinear coordinate measured along the streamline between inlet and outlet, then after previous calculus for N discrete points, indexed with i (i=0…N) the following data are known: r_i, z_i, x_i, β_i, φ_i. For the construction of the camber line in the conformal mapping plan, ΔA_i is determined using the equation:

$$\begin{aligned} &\Delta A_i = \frac{r_i + r_{i-1}}{2}(\varphi_i - \varphi_{i-1}) \\ &\Rightarrow \quad A_i = \sum_{i=0}^{i} \Delta A_i \end{aligned} \tag{9}$$

On the Y axis Lm_i is plotted:

$$Lm_i = \sum_{i=0}^{i} \Delta Lm_i = \sum_{i=0}^{i} \Delta x_i = \sum_{i=0}^{i} (x_i - x_{i-1}) \tag{10}$$

The thickness function is introduced towards the camber line. For the impeller this function is of constant thickness and only for the leading edge is profiled. If s is the thickness of the blade, then the offset curve that bounds the camber line is determined for the pressure side and suction side with the equations:

$$\begin{cases} A_{ps_i} = A_i + \dfrac{s}{2}\sin\beta_i \\ L_{ps_i} = Lm_i - \dfrac{s}{2}\cos\beta_i \end{cases} \tag{11}$$

$$\begin{cases} A_{ss_i} = A_i - \dfrac{s}{2}\cos\beta_i \\ L_{ss_i} = Lm_i + \dfrac{s}{2}\sin\beta_i \end{cases} \tag{12}$$

On the leading edge the profile is made with ellipse arcs connected with the offset lines of the transpose thickness. If a and b are the semi-axes of the ellipse then the coefficient $k_e = a/b$ is introduced and becomes a control parameter of the leading edge profile, and b will be $b = s/2$. Depending on the curved coordinate x_{cl} (x along the camber line) in the local coordinate system (Figure 5), the coordinates are determined with the equations:

$$\begin{cases} x_M = k_e \dfrac{s}{2} - x_{cl} \\ y_M = \dfrac{1}{k_e}\sqrt{\left(k_e \dfrac{s}{2}\right)^2 - x_M} \end{cases} \tag{13}$$

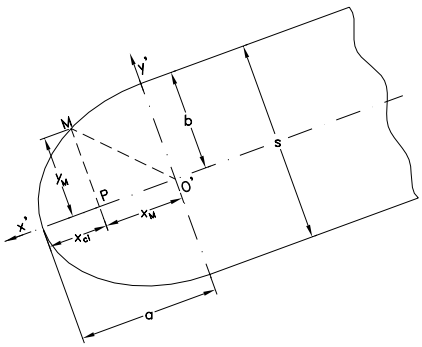

Fig. 5. Leading edge profile with ellipse arcs

This method of profiling the leading edge is valid only for impeller blade of constant thickness. On the trailing edge the blade is cut off. This model is tested in the first phase of the study and in the future the trailing edge will be profiled or cut off after a circle with the radius equal with the outlet radius. In figure 6 the result of this phase of the study is presented:

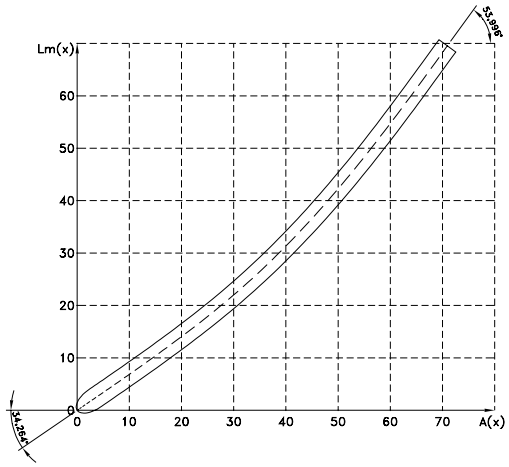

Fig. 6. The profile of the blade of constant thickness in the conformal mapping plane

Using the same method for all the calculus sections all the profiles are obtained as presented in the Figure 7.

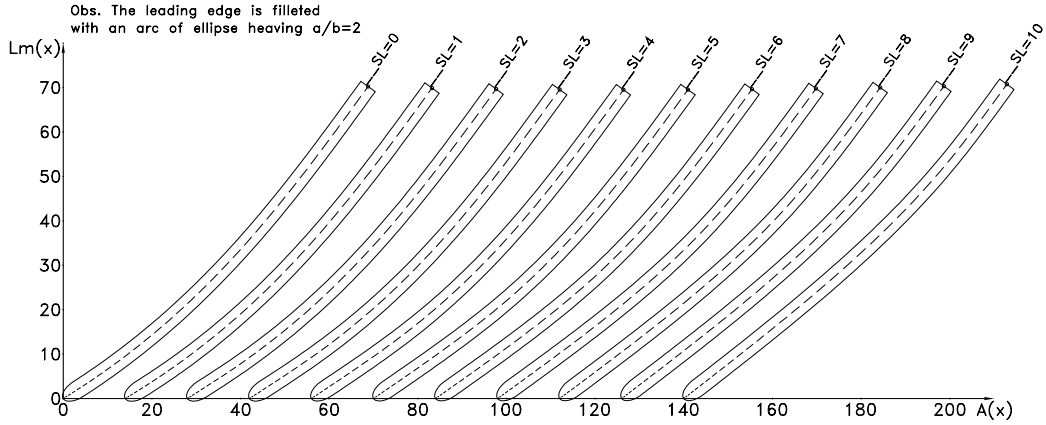

Fig. 7. The streamlines and their hydrodynamic profiles in the conformal mapping plan for all sections for the impeller with n_q=18.18

It can be observed that the shape of the camber line is very much alike with the shape generated directly in the conformal mapping plane, and has no inflexions and it is monotone increasing between inlet and outlet. This aspect suggests the possibility to couple the optimisation of the blade shape through the classic method with the method of the conformal transpose.

6. TRANSPOSITION OF THE GEOMETRIC DATA OF THE IMPELLER BLADE FROM THE CONFORMAL MAPPING PLAN ON THE STREAM SURFACES

The images of the blade profile from the conformal mapping plane have an identical correspondent on the stream surfaces from where the camber lines come. The transposition is made on small consecutive intervals, which were obtained from the meshing of the surface between inlet and outlet.

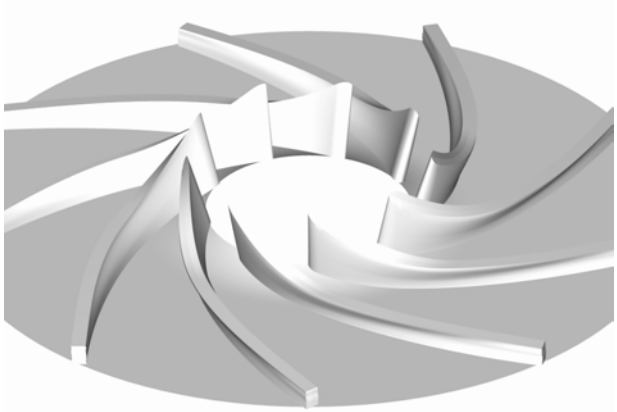

Fig. 8. 3D image of the impeller blades (the band surface was removed)

The coordinates (r,φ,z) of the points are obtained through linear interpolation.

The examination of the results is made with AutoCAD, using a script file which generates mesh surfaces. Through rotation, zooming and rendering the precision of the images is studied as shown in Figure 8.

After everything is checked and validated the files with extension *.jou are generated and with these files the coordinates of the boundary surfaces from the crown and band, of the surface of the blade camber (for the definition of the periodic boundary) and of the surface of the blade is imported in GAMBIT and FLUENT. These are the initial data for the procedure needed for the numerical simulation of the flow.

7. 3D COMPUTATIONAL DOMAIN AND MESH

Computerized pump design has become a standard practice in industry, and it is widely used for both new designs as well as for old pumps retrofit. Such a complex design code has been developed over the past decade by the first author. However, any design method has to accept a set of hypotheses that neglect in the first design iteration the three-dimensional effects induced by the blade loading, as well as the viscous effects. As a result, an improved design can be achieved only by performing a full 3D flow analysis in the pump impeller, followed by a suitable correction of the blade geometry and/or the meridian geometry.

Although GAMBIT has a module, called G-TURBO, specialized in turbomachinery analysis, it has been found that for highly distorted geometries specific to axial-radial machines the results are not satisfactory. This is why we developed an original procedure that successfully addresses all geometrical particularities of centrifugal pumps.

Consequently, a fully automatic procedure for generating the inter-blade channel 3D geometry for impeller, starting with the geometrical data provided by the quasi- 3D code is implemented. The 3D computational domain is generated in GAMBIT [6] with a specialized script (journal file). The journal file (*.jou) generates automatically the 3D computational domain for inter-blade channel of impeller in GAMBIT. Next, the boundary conditions on the surfaces are specified for a standard topology of the inter-blade channel. Then, the 3D computational domain is automatically discretized.

In this paper, three impellers are designed in order to evaluate our procedure. The hydrodynamic parameters of the impellers are presented in Table 1.

Table 1.

No.	Q [m^3/h]	H m]	n [rpm]	n_q	z
1	50	50	2900	18.18	9
2	200	35	2900	47.50	8
3	1000	15	1450	100.26	11

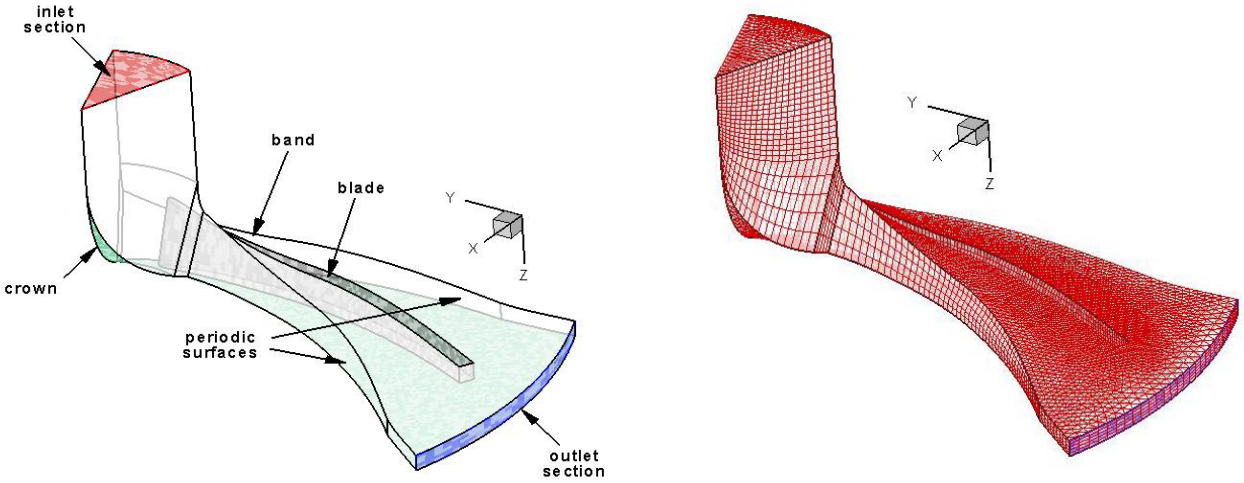

Fig. 9. 3D computational domain and mesh on the channel of the impeller with n_q=18.18

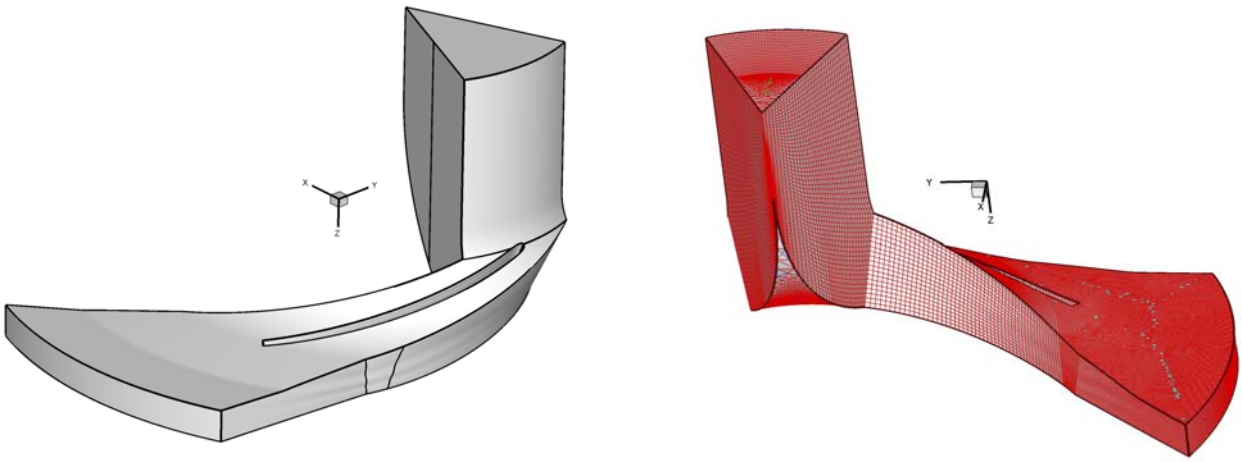

Fig. 10. 3D computational domain and mesh on the channel of the impeller with n_q=47.50

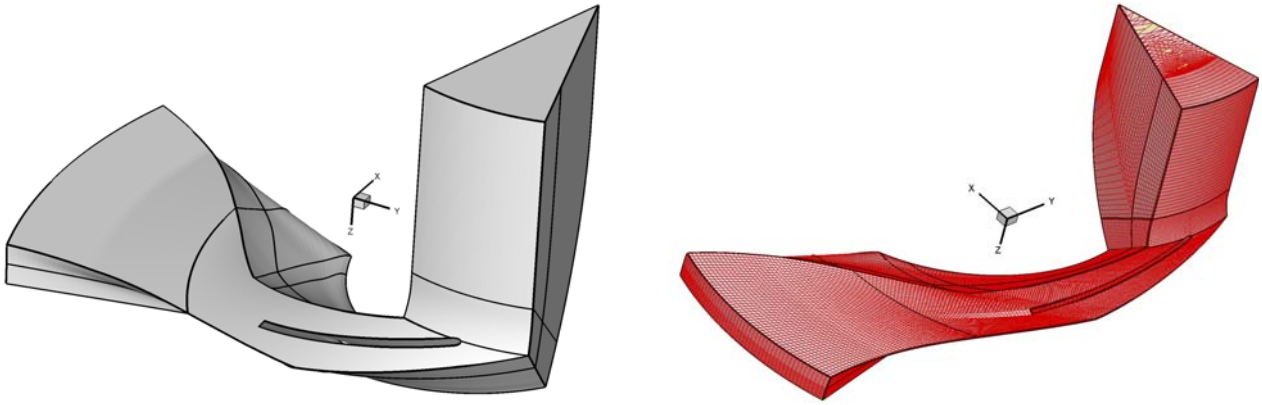

Fig. 11. 3D computational domain and mesh on the channel of the impeller with n_q=100.26

8. 3D NUMERICAL INVESTIGATION OF THE FLOW THROUGH PUMP IMPELLERS

For the flow analysis presented in this paper we consider a 3D Euler flow model. Consequently, the cavitational behaviour of the designed impellers is evaluated. A steady relative 3D Euler flow is computed using following equations,

$$\nabla \cdot W = 0 \tag{14a}$$

$$\frac{d(\rho \mathrm{W})}{dt} = \rho \mathrm{g} - \nabla p \tag{14b}$$

The numerical solution of flow equations (14a) and (14b) is obtained with the expert code FLUENT 6.0. [7]. The Euler solution will be used like an initial solution for turbulent computation.

The $NPSH_r$ (N*et* P*ositive* S*uction* H*ead* r*equired*) is defined as:

$$NPSH_r = \left(\frac{p_{inlet}}{\rho g} + \frac{W_{inlet}^2}{2g} \right) - \frac{p}{\rho g} \tag{15}$$

where the variables correspond to the averaged one on inlet section of the impeller.

In Figures 12-14(left) the $NPSH_r$ distribution on the blades is plotted for all impellers investigated. One can see the $NPSH_r$ maximum value for each impeller is obtained at the junction between crown and blade suction side, see the red spots in Figs. 12-24(right). The red spots indicate the regions with maximum risk at cavitation development. However, keeping in mind that all numerical analysis were performed at best design point (BDP)

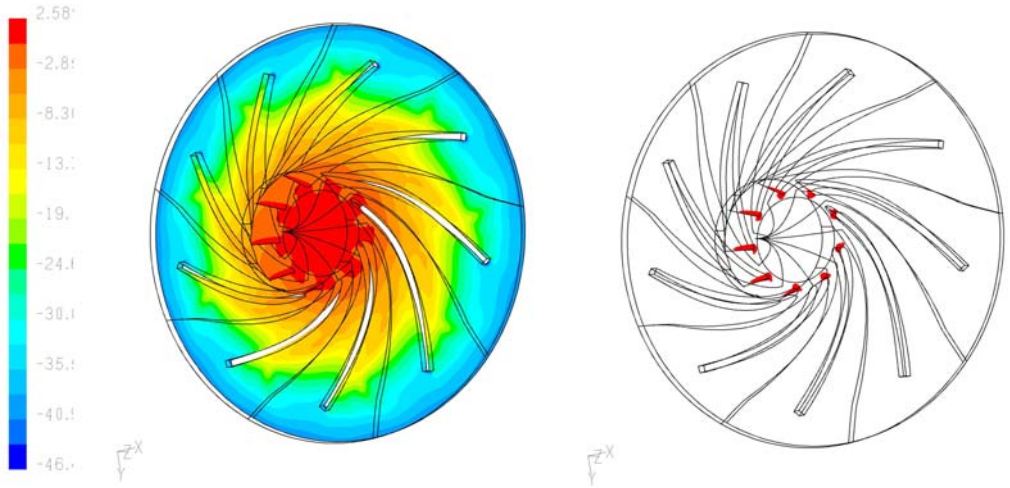

Figure 12. $NPSH_r$ distribution on the impeller with n_q=18.18 (left). The red spots indicate maximum risk at cavitation development (right).

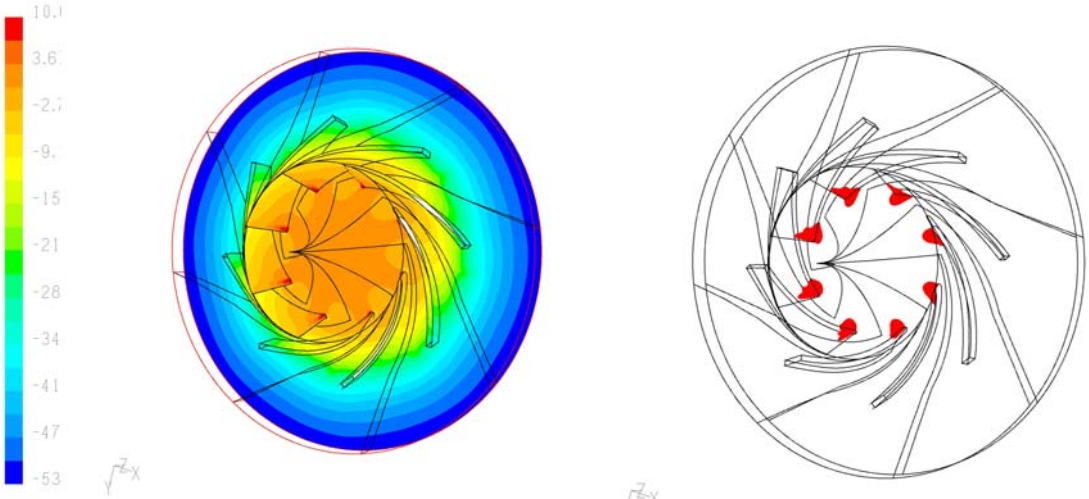

Figure 13. $NPSH_r$ distribution on the impeller with n_q=47.50 (left). The red spots indicate maximum risk at cavitation development (right).

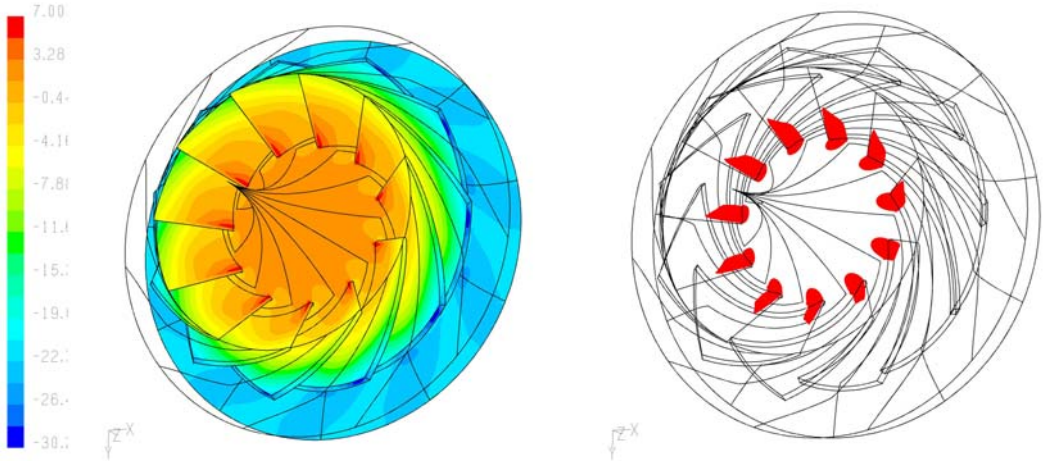

Figure 14. $NPSH_r$ distribution on the impeller with n_q=100.26 (left). The red spots indicate maximum risk at cavitation development (right).

9. CONCLUSIONS

The present paper presents a fully automated procedure for generating the inter-blade channel 3D geometry for centrifugal pump impeller, starting with the geometrical data provided by the quasi- 3D code. The 3D domain is generated in GAMBIT with a specialized script, and then it is automatically discretized. All inlet/outlet, solid and periodic boundaries are specified for a standard topology of the inter-blade channel. Although GAMBIT has a module, called G-TURBO, specialized in turbomachinery analysis, it has been found that for highly distorted geometries specific to axial-radial machines the results are not satisfactory. This is why we developed an original procedure that successfully addresses all geometrical particularities of centrifugal pumps. The paper describes the implementation of our procedure, and three examples of 3D flow analysis in centrifugal pump impellers.

REFERENCES

1. Radha Krishna H.C. (ed.), (1997) *Hydraulic Design of Hydraulic Machinery*, Avebury Publishing House.
2. Gyulai Fr., (1988) *Pumps, Fans, Compressors*; vol I & II, Politehnica University Publishing House, Timişoara.
3. Pfleiderer K., (1961) *Die Kreiselpumpen für Flüssigkeiten und Gase*, Springer Verlag, Berlin.
4. Anton L.E., Miloş T., (1998) *Centrifugal Pumps with Inducer*, Orizonturi Universitare Publishing House, Timişoara, Romania.
5. Miloş T., (2002), *Computer Aided Optimization of Vanes Shape for Centrifugal Pump Impellers*, Scientific Bulletin of the "Politehnica" University of Timişoara, Romania, Tom 47(61).
6. Fluent Inc., (2001) *Gambit 2. User's Guide*, Fluent Incorporated.
7. Fluent Inc., (2001) *FLUENT 6. User's Guide*, Fluent Incorporated.